Effect of a Single Applied Overload on Fatigue Crack Growth Behavior in Laser-welded Sheet Metal

Dai-Soon Kwak[1], Seog Hwan Kim[1] and Taek Yul Oh[2,#]

1 Graduate School of Mechanical Engineering, Kyunghee University, Yongin, South Korea
2 College of Advanced Technology, Kyunghee University, Yongin, South Korea
Corresponding author / E-mail: tyoh@khu.ac.kr, Tel: +82-31-201-2977; Fax: +82-31-202-8106

KEYWORDS : Fatigue crack, Overload, Laser weld, Plastic zone, Crack growth rate, Stress intensity factor, Nanoindentation

We investigated fatigue crack growth behavior in laser-welded sheet metal caused by a single applied overload. The fatigue specimens were made using butt jointed cold rolled sheet metal that was welded with a CO_2 laser. The effects of the specimen thickness and overload ratio were determined from fatigue crack propagation tests. These tests were performed in such a way that the fatigue loading was aligned parallel to the weld line while the crack propagated perpendicular to the weld line. Overload ratios of 1.0, 1.5, and 2.0 were applied near the tip of the fatigue crack at points located 6, 4, and 2 mm from the weld line. The specimens were either 0.9 or 2.0 mm thick. The size of the plastic zone at the crack tip due to the single applied overload was also determined using finite element analysis.

Manuscript received: August 4, 2005 / Accepted: December 16, 2005

1. Introduction

Laser welding techniques have several advantages over conventional methods. In addition to their very fast welding speed, the laser penetrates deep into the specimens and produces small deformations due to the narrow heating zone, without mechanical contact with the specimens during the process. Due to the high-density energy, laser welding can be used to join heterogeneous materials.[1,2] Therefore, laser welding has recently become a popular method for tailored blank technology in which different materials are welded through one-step press forming. This is especially true for automobile body panels, in which laser welding is used to form materials with different strengths and coatings. It is an attractive method because it can produce a light body with fine precision in a highly productive environment. [3]

Intensive research has been conducted to determine the optimal welding conditions required to improve the formability and structural stability of laser-welded specimens.[4-6] Most research into the structural stability has been related to the evaluation of the stress around the welding zone; only a small number of studies have considered the fatigue characteristics of laser-welded structures. [7-9] In particular, it is difficult to find studies that focus on the fatigue behavior of laser-welded structures subjected to a single applied overload, a situation often encountered in practical applications. Therefore, in this study, laser-welded specimens were used to investigate fatigue crack growth behavior during a single applied overload. The tests were performed by applying the overload at various locations using different overload ratios (overload / applied load) and specimen thicknesses. The stress and plastic zone around crack tip were investigated using a finite element method. Since the weld bead produced by laser welding is only 1.0 mm and therefore very narrow, it can be difficult to measure the mechanical properties of welded specimens at the weld bead in the heat-affected zone (HAZ). This problem was overcome by using nanoindentation tests. The results from these tests were then supplied as input parameters for the finite element analysis.

2. Experiment and Analysis

2.1 Specimen preparation and welding conditions

The material used in this study was SPCEN (KS D 3512) sheet metal. The chemical composition of SPCEN is listed in Table 1. The laser welding was performed using a CO_2 laser in a Helium (He) gas environment. The welding power was 4 kW and the welding speed was 6 m/min. Fig. 1 shows a schematic diagram of the fatigue crack propagation in a test specimen that contained a 13-mm-long pre-crack at its edge. The pre-crack was made using a wire cutting machine.

Table 1 Chemical composition of SPCEN (percent weight)

Element	C	Mn	Si	P	S
%	0.016	0.19	0.029	0.019	0.006

Table 2 shows the mechanical properties of the base metal and laser-welded specimens. The tensile strength of the base metal specimen was 339 MPa, while that of the laser-welded specimen was 374 MPa. Thus, the tensile strength of the laser-welded specimen was 10% greater than that of the base metal specimen.

Copyright (c) 2006 by KSPE

Table 2 Mechanical properties of the base metal and laser-welded specimens

Specimen	Yield Strength [MPa]	Tensile Strength [MPa]	Elongation [%]
Base metal	215.7	339.3	39
Laser-welded*	261.3	374.2	25

* Loading direction was parallel to the weld line

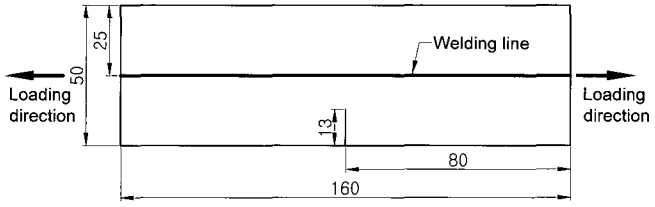

Fig. 1 Schematic diagram of a test specimen

2.2 Fatigue crack propagation test

Fatigue crack propagation tests were performed using a servo hydraulic fatigue-testing machine. The tensile fatigue load (stress ratio R = 0) was applied parallel to the welding direction at room temperature. The load form was sinusoidal and the loading frequency was 10 Hz. First, a single overload (overload ratio = 2.0) was applied to a base metal specimen and a laser-welded specimen at a crack length of 21 mm to investigate the effect of the applied overload on the fatigue behavior. Then overloads (overload ratio = 2.0) were applied to fresh specimens at crack lengths of 19, 21, and 23 mm to investigate the effect of the applied overload location on the crack retardation rate. These positions were located 6, 4, and 2 mm from the weld line, respectively. Three different overload ratios (1.0, 1.5, and 2.0) were also applied to fresh specimens at a crack length of 21 mm to investigate the effect of the overload ratio on the crack propagation rate. Finally, 0.9- and 2.0-mm-thick specimens were laser-welded to investigate the effect of the specimen thickness on the fatigue behavior of resulting structure. The crack lengths were measured based on the ASTM E647 standard under a 100× traveling microscope with a CCD camera.

2.3 Nanoindentation test

Continuous nanoindentation tests were performed to measure the elastic modulus around the weld zone. Fig. 2 illustrates the measurement direction and the tested locations, which were separated by 0.05 mm, on each specimen. Fig. 3 shows the MTS Nano Indenter/XP used for this test.

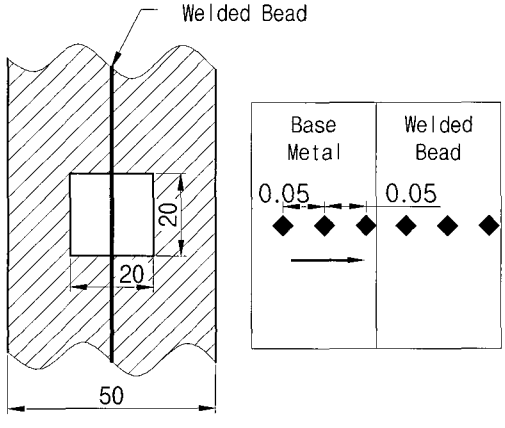

Fig. 2 Schematic diagram for the nanoindentation tests

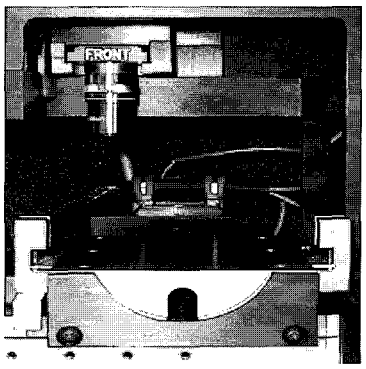

Fig. 3 MTS Nano Indenter/XP

2.4 Finite element analysis

A finite element analysis was performed using the ABAQUS program to analyze the stress distribution and plastic zone shape near the crack tip. The base metal, weld bead, and heat-affected zone were modeled separately, and the material properties determined from the nanoindentation tests were used as the input data.

3. Results and Discussion

3.1 Fatigue crack propagation

Fatigue crack propagation tests were performed to investigate the fatigue behavior of welded metal due to an applied overload. Fig. 4 shows a comparison of the fatigue behavior of base metal and welded specimens when an overload was applied at a crack length of 21 mm. For the base metal case, the crack propagated normally until the crack length reached 21 mm. Then the crack propagation rate started to retard. The crack propagation behavior was similar for the welded specimen case until the crack reached the weld bead. However, the crack propagation rate decreased dramatically when the crack passed through the weld bead due to the increased strength at the weld bead and the compressive stress caused by the applied overload.

An overload ratio of 2.0 was applied to fresh specimens at crack lengths of 19, 21, and 23 mm to investigate the effect of the applied overload location on the fatigue behavior. The results are shown in Fig. 5. With an applied overload at a crack length of 19 mm, the crack propagation rate was retarded until the crack was 22 mm long, after which the propagation rate increased until the crack reached the weld bead. The crack then propagated quickly through the weld bead and resumed its normal propagation speed. With an applied overload at 21 mm, the crack propagation rate was continuously retarded until the crack reached the weld bead. There was a major decrease in the crack propagation rate through the weld bead; then the crack propagation rate increased and resumed its normal speed in the base metal. A similar behavior was observed when the overload was applied at a crack length of 23 mm. As the overload was applied closer to the weld bead, the derivative of the retarded crack propagation rate in the weld bead increased quickly while the derivative of resumed crack propagation rate in the base metal increased slowly. The retarded crack in the 23-mm case was 5% larger than that in the 21-mm case, and 14% larger than that in the 19-mm case. The crack propagation rate near the weld bead was a minimum for the 21-mm case and a maximum for the 23-mm case. The minimization of the crack propagation rate for the 21-mm case was attributed to the strength discontinuity and residual stresses at the weld bead.

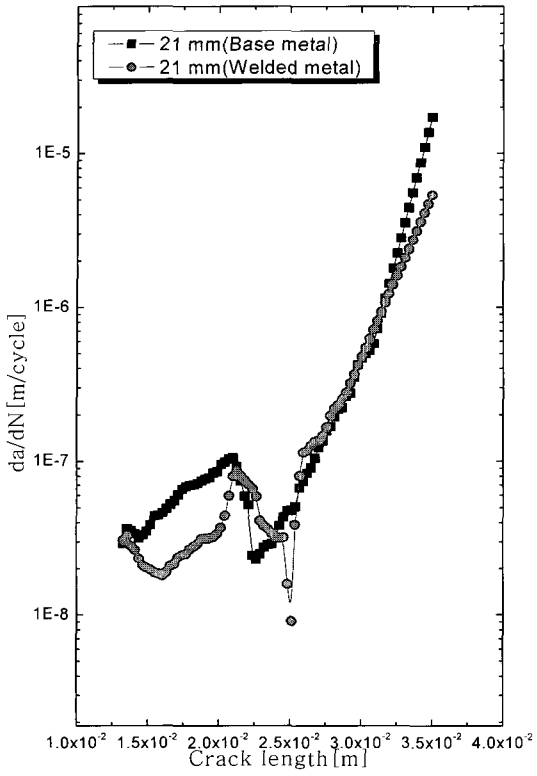

Fig. 4 Effect of the crack length on fatigue crack propagation for the base metal and welded specimens

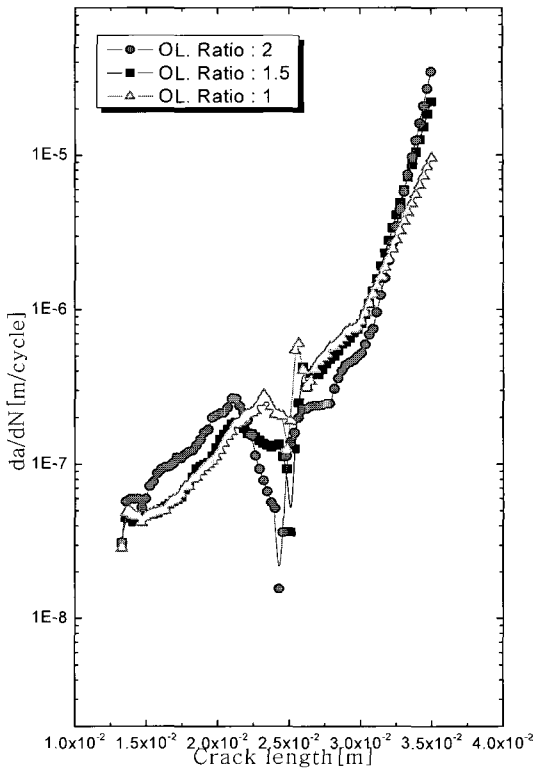

Fig. 6 Effect of the overload ratio on the fatigue behavior of the welded specimen

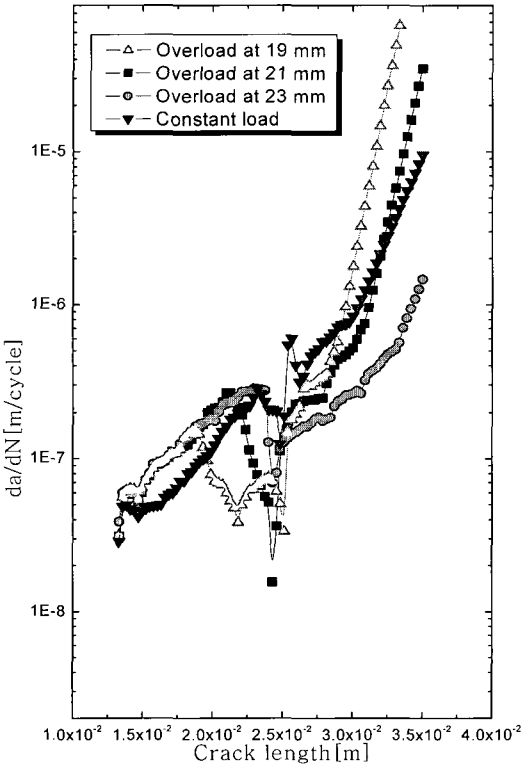

Fig. 5 Effect of the overload location on the crack length

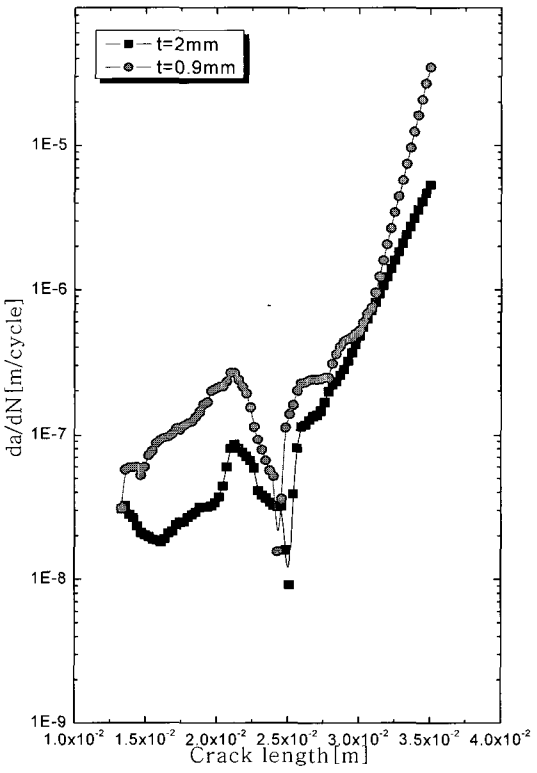

Fig. 7 Effect of thickness on the fatigue behavior of the welded specimen

Three different overload ratios were applied at a crack length of 21 mm to determine the effect on the crack propagation behavior. The applied overload ratios were 1.0, 1.5, and 2.0. The results are shown in Fig. 6. Irrespective of the overload ratio, the crack propagation rate was retarded after the location of the applied overload and decreased sharply near the weld bead. The cracks propagated quickly through the weld bead and resumed their normal propagation rates in the base metal. The figure also shows that the crack propagation rate decreased with increasing overload ratio.

An overload ratio of 2.0 was applied at a crack length of 21 mm to the 0.9- and 2.0-mm-thick specimens to determine the effect on the crack propagation behavior. The results are shown in Fig. 7. The crack propagation rate was retarded after the crack passed the applied overload; the crack propagation rate decreased sharply near the weld bead for both specimens. Then the crack propagation rate increased sharply in the weld bead. The crack propagation rate of the thicker specimen was less than that of the thinner specimen. The decrease in the crack propagation rate was also less in the thicker specimen.

3.2 Nanoindentation

Fig. 8 shows typical load-displacement curves for the laser-welded sheet metal specimens determined from the nanoindentation tests. The load-displacement curves varied depending on the base metal, welded bead, and the HAZ. Fig. 9 shows the elastic modulus variation as a function of location. In general, the small weld bead produced by laser welding in this study was approximately 1 mm. The elastic modulus of the base metal was 191 GPa, similar to that in the tensile test. The HAZ corresponded to about 1 mm of base metal on either side of the bead. The elastic modulus of the HAZ was 220 Gpa, while that of the weld bead was 238 GPa.

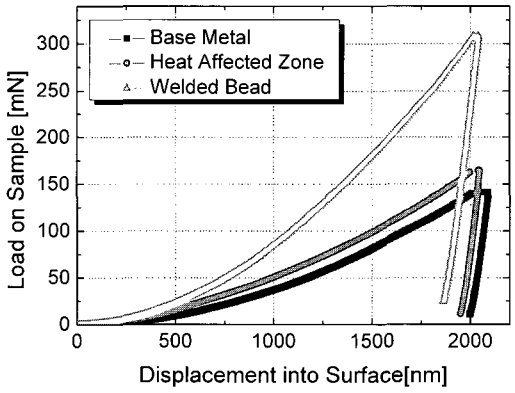

Fig. 8 Load-displacement curve of a laser-welded specimen

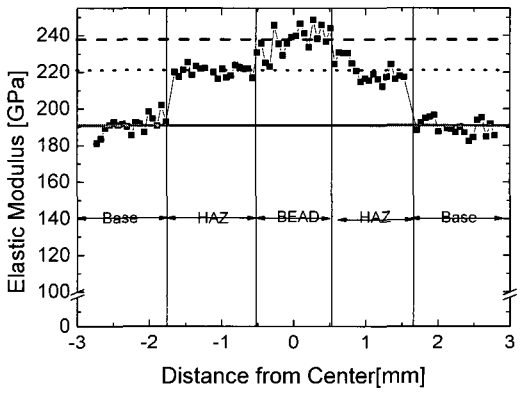

Fig. 9 Elastic modulus variation in the base metal, HAZ, and weld bead

3.3 Size of the plastic zone and stress analysis

A finite element analysis was performed using the ABAQUS program to determine the size of the plastic zone and stress distribution near the crack tip. The material properties determined from the nanoindentation tests were used as input data and perfectly plastic behavior was assumed. Fig. 10 shows the finite element modeling with the HAZ encompassing 1 mm of base metal on either side of the bead. Fig. 11 shows the stress distribution at the crack tip for a crack length of 21 mm when the applied load was equal to the fatigue load. For this case, high stresses were predicted for the HAZ and bead because the strength of these regions was increased by the laser-welding process. Fig. 12 shows the shape of the plastic zone obtained for the unloaded condition after the following overload ratios were applied: (a) 1.0, (b) 1.5, and (c) 2.0. The plastic zone extended 1.7 mm in the crack propagation direction for an overload ratio of 1.5 and 2.5 mm in the crack propagation direction for an overload ratio of 2.0. The size of the plastic zone was related to the intervals of crack retardation shown in Fig. 6. When the applied overload ratio was 1.5, the crack was retarded in the plastic zone while a constant crack propagation rate was maintained after the plastic zone. Then the crack was retarded again until it reached the weld bead due to the increased strength of this region. When the applied overload ratio was 2.0, the crack was continuously retarded until it reached the weld bead because the plastic zone was larger and extended to the front of weld bead.

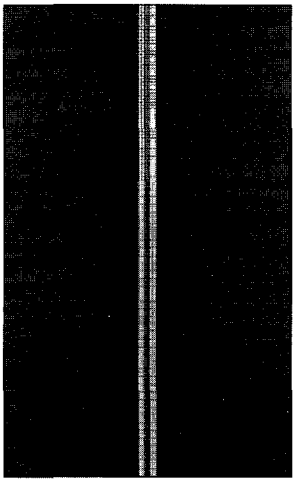

Fig. 10 Finite element analysis modeling

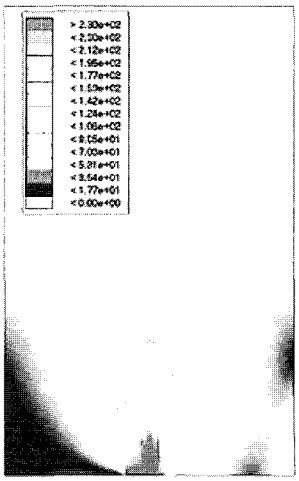

Fig. 11 Von Mises stress distribution at the crack tip for a crack length of 21 mm

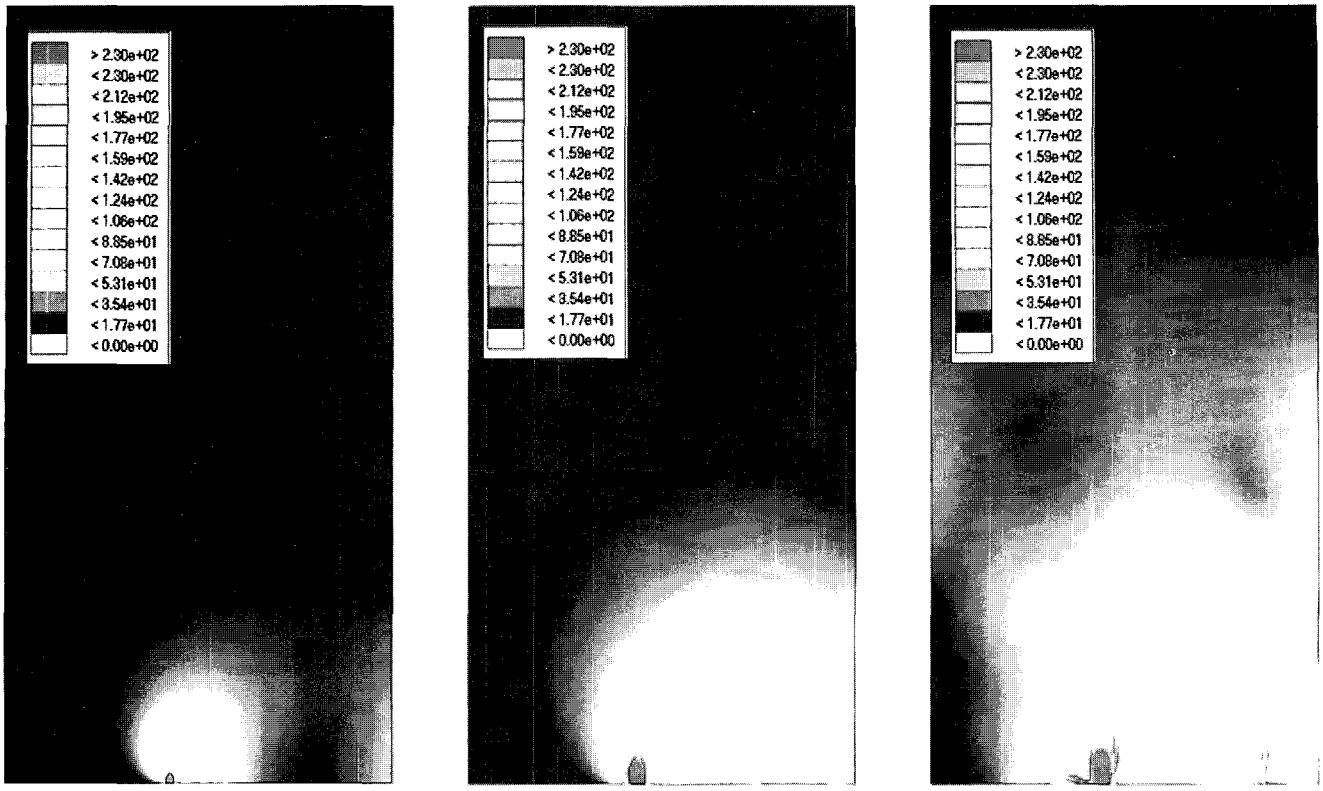

(a) Overload Ratio = 1.0 (b) Overload Ratio = 1.5 (c) Overload Ratio = 2.0

Fig. 12 Shape of the plastic zone in the unloaded condition after the overload was applied

4. Conclusions

We investigated the fatigue crack growth behavior of laser-welded sheet metal after a single overload was applied. A finite element analysis was performed to determine the stress distribution and size of the plastic zone at the crack tip. The following conclusions were obtained.

1) The values of the elastic modulus in the HAZ and weld bead were 12.8 and 20.0% greater than that of base metal, respectively.

2) The effect of the applied overload on the crack retardation in the laser-welded specimen was greater than that of the base metal. The large crack retardation occurred due to the increase in strength at the weld bead.

3) The crack retardation behavior of the thinner specimen was markedly greater than that of the thicker specimen.

4) The size of the plastic zone determined from the finite element analysis corresponded well with the interval at which the crack propagation rate was retarded after the overload was applied.

ACKNOWLEDGEMENT

This work was supported by project R05-2003-000-11383-0 funded by the Korea Science and Engineering Foundation (KOSEF).

REFERENCES

1. Prange, W., Schnelder, C. and Sellge, A. J., "Application of Laser-Beam-Welded Sheet Metal," SAE 890853.

2. Selige, A. J. and Prange, W., "Production and Usage of Laser Beam Welded Sheet Metal," SAE 970413.

3. Lee, A. P., Feltham, E. and Deventer, J., "Tailor Welded Blank Technology for Automotive Applications," SAE 960817.

4. Eisenmenger, M., Bhatt, K. K. and Shi, M. F., "Influence of Laser Welding Parameters on Formability and Robustness of Blank Manufacturing: An Application to a Body Side Frame," SAE 950922.

5. Martukanitz, R. P., Altshuller, B., Armao, F. G. and Pickering, E. R., "Properties and Characteristics of Laser Beam Welds of Automotive Al Alloys," SAE 960168.

6. Potente, H. and Becker, F., "Weld Strength Behavior of Laser Butt Welds," ANTEC, 1999.

7. Hwang, J. R., Doong, J. L. and Chen, C. C., "Fatigue Crack Growth in Laser Weldments of a Cold Rolled Steel," Materials Transactions, JIM, Vol. 37, No. 8, pp. 1443-1446, 1996.

8. Wang, B. Y., Shi, M. F., Sadrnia, H. and Lin, F., "Structural Performance of Tailor Welded Sheet Steels," SAE 950376.

9. Rhee, K. Y., Kwak, D. S. and Oh, T. Y., "Fatigue Behavior Characterization of Laser-welded Cold Rolled Sheet Metal (SPCEN)," Journal of Materials Science, Vol. 37, pp. 1019-1025, 2002.

10. Choo, B. Y. and Keum, Y. T., "Evaluation of Mechanical Properties of Welded Metal in Tailored Steel Sheet Welded by CO_2 Laser," Journal of Korean Society of Precision Engineering, Vol. 18, No. 4, pp. 142-150, 2001.